Applied Physics B (2020) 126:171
https://doi.org/10.1007/s00340-020-07521-5

Applied Physics B
Lasers and Optics

Laser synthesis of 2D structures for photo-thermo sensors with high sensitivity

N. Stefan[1] · S. A. Mulenko[2] · M. A. Skoryk[2] · V. M. Popov[3] · O. Yo. Gudymenko[4]

Received: 10 April 2020 / Accepted: 17 September 2020

Abstract
Semiconductors are considered as promising materials for the fabrication of photo-thermo sensors with high sensitivity. Therefore, here we propose to synthesize of amorphous 2D single-layered structures with high thermo-photosensitivity by using photons generated by a KrF* laser radiation ($\lambda = 248$ nm, $\tau_{FWHM} \leq 25$ ns) in the reaction of copper (Cu) atoms with methane (CH_4) molecules by reactive pulsed laser deposition (RPLD) process. Optimum conditions were found out to synthesize of these structures with the thickness of (56–160) nm. X-ray diffraction analysis evidenced either amorphous or polycrystalline structures on the deposits. Element analysis was carried out by energy-dispersive X-ray spectroscopy (EDXS). The semiconductor temperature trend was detected with the variable energy band gap (E_g) in the range of (0.17–1.0) eV depending on substrate temperature, CH_4 pressure and structures' thickness. The highest photosensitivity of these structures was high as 640 V/W at white light power density ~ 6×10^{-3} W/cm^2 and the highest thermo-sensitivity (Seebeck coefficient) was high as 10.5 mV/K. An interpretation is provided for thermo-photosensitivity behaviour. The amorphous 2D single-layered structures were synthesized by laser radiation for the first time with such superior thermo-photo properties. Therefore, such structures are exceptional candidates for a new generation of effective thermo-photo sensors operating at moderate temperatures.

1 Introduction

A great interest is nowadays focused on 2D structures to test the advantages of thin films on the performances of electronic devices and sensors [1]. As it was shown, thin films (2D structures) based on transition metals silicides and oxides synthesized by pulsed laser deposition (PLD), reactive pulsed laser deposition (RPLD), and laser chemical vapour deposition (LCVD) can be considered a challenging opportunity for new thermo-tenso-photo-chemical sensors [2–8]. The silicides and oxides demonstrated semiconductor properties characterised with an energy band gap (E_g) less than 1.0 eV. RPLD was first applied for the synthesis of iron oxide 2D structures on <100> Si substrate for thermo-chemical sensors [3, 7, 8]. Nevertheless, one still meets a major difficulty with white light spectrum energy conversion, in particular, solar energy conversion into an electrical one. Semiconductor materials with a variable band gap open new approaches for converters in comparison with the single band gap ones. Semiconductor materials based on Cu(In,Ga)(Se,S)$_2$ structures were synthesized with a variable band gap from 1.04 to 1.7 eV in the case of In/Ga and Se/S content [9, 10]. In the context, one should remember the

✉ S. A. Mulenko
mulenko@ukr.net

N. Stefan
stefan.nicolaie@inflpr.ro

M. A. Skoryk
skoryk@nanomedtech.com

V. M. Popov
vmpopov7777@gmail.com

O. Yo. Gudymenko
gudymen@ukr.net

[1] National Institute for Lasers, Plasma and Radiation Physics, PO Box MG-54, 77125 Magurele, Romania

[2] G. V. Kurdyumov Institute for Metal Physics NAS of Ukraine, 36, Academician Vernadsky Blvd., Kyiv 03142, Ukraine

[3] State Enterprise "Research Institute of Microdevices" STC "Istitute for Single Crystals", NAS of Ukraine, 3, Severo-Syretska, Kyiv 04136, Ukraine

[4] V. F. Lashkaryov Institute of Semiconductor Physics, NAS of Ukraine, 41, Prospect Nauki, Kyiv 03028, Ukraine

Published online: 03 October 2020

historical discovery by Charles Edgard Frits in 1883, which created a wide plate of copper, doped with Se and covered with an extremely thin semi-transparent layer of gold to generate electrical current. As it is known, chromium oxide thin films (2D structures) with a stoichiometry $Cr_{3-X}O_{3-Y}$ ($0 \le X \le 2$; $0 \le Y \le 2$) proves a great interest for application in solar energy converters into electricity [11].

There are major problems concerning for materials with high thermo-sensitivity (Seebeck coefficient, *S*), mainly due to the connection with thermo-sensor and energy conversion. There are some publications devoted to 2D structures and thicker layers with a relatively high *S* coefficient. High Seebeck coefficient of 0.85 mV/K was reached with two-dimensional electron gas of $SrTiO_3$ structures [12]. The *S* coefficient not higher than 0.10–0.20 mV/K at 300 K was obtained for PbTe bulk samples synthesized by using a molecular beam epitaxy (MBE). Adding Se to PbTe ($PbSe_{0.5}Te_{0.5}$) resulted in *S* coefficient increasing up to 0.25 mV/K [13]. Relatively high coefficient $S \cong 0.30$ mV/K at 973 K was achieved in *β*-phase copper selenide (Cu_2Se) polycrystals synthesized by hot-pressing method [14]. Copper oxides CuO, Cu_2O with 0.7–1.3 µm thickness demonstrated the *S* coefficient in the range 0.90–0.20 mV/K at room temperature (*RT)* while the deposition of the copper target in oxygen-argon atmosphere on sapphire substrate by a radio frequency (RF)-sputtering [15].

Data concerning *S* coefficient and photosensitivity (*F)* reported in previous papers are collected in Table 1.

Our option is based on our experience of iron and chromium oxides 2D structures synthesis by RPLD using a KrF^* laser radiation [3, 4, 7, 16–19]. Before, the synthesized 2D structures with high thermo-photosensitivity were received on single and multi-layered polycrystalline $Fe_2O_{3-X}/Cr_{3-X}O_{3-Y}$ 2D structures [16–19]. On the other hand, some materials with relatively high thermo-sensitivity were synthesized using toxic precursors' atoms such as Te, Se, Pb, and Sr (Table 1). But up-to-date material technology should be based on non-toxic precursors as the background of "green" technologies. Therefore, the aim of this work is the application of KrF^* laser radiation for the synthesis of amorphous 2D single-layered structures materials with high thermo-photosensitivity based on non-toxic precursors and element composition of 2D structures' influence on their thermo-photosensitivity. Here we propose to synthesize of the 2D single-layered structures with high thermo-photosensitivity based on the reaction of Cu atoms with CH_4 molecules by using RPLD. The experimental conditions were investigated to provide the best values to these important S_{max} and F_{max}. parameters. An interpretation is provided about the behaviour of high thermo-photosensitivity of these 2D single-layered structures.

2 Experimental procedures

2.1 Synthesis of 2D structure

As it is known, RPLD is quite suitable for the synthesis of 2D structures with high purity and well-defined stoichiometry [2–4, 6, 7]. In present experiments, pure Cu (99.5%) target was ablated with a KrF* ($\lambda = 248$ nm, $\tau_{FWHM} \le 25$ ns) excimer laser radiation, at a fluence of (4.0–4.5) J/cm^2 and a frequency repetition rate of 10 Hz in a stainless-steel vacuum reactor in the ambiance of a CH_4 atmosphere. Before

Table 1 S_{max} coefficient and F_{max} parameter for different structures: relevant data were reported in previous papers

Material	Type of structure	Synthesis methods	S_{max}, (mV/K)	F_{max}, (V/W)	Temperature range, (K)	References
β-phase $FeSi_2$	2D	PLD	1.5	–	100–340	[2]
$CrSi_2$	2D	PLD	1.4	–	220–340	
$Fe_2O_{3-X}(0 \le X \le 1)$	2D	RPLD	1.65	–	293–322	[3]
$Cr_{3-X}O_{3-Y}(0 \le X \le 2; 0 \le Y \le 2)$	2D	RPLD	3.5–4.5	–	270–290	[4]
$Fe_2O_{3-X}(0 \le X \le 1)$	2D	LCVD	1.5–1.6	40	260–290	[7]
	2D	RPLD	1.65	43	260–300	
$SrTiO_3$	2D	Thermal annealing	0.85	–	85–300	[12]
PbSe, PbTe, $PbSe_{0.5}Te_{0.5}$	Bulk (lead-salt)	MBE	0.10–0.20 0.25	–	300	[13]
β-phase Cu_2Se	Bulk polycrystals	Hot-pressing	0.30	–	973	[14]
Cu_XO $1 \le X \le 2$	(0.7–1.3) µm polycrystals	RF-sputter deposition	0.90–0.20	–	293	[15]
$Cr_{3-X}O_{3-Y}(0 \le X \le 2; 0 \le Y \le 2)$	2D	RPLD	8.0	–	280–330	[16]
$Fe_2O_{3-X}(0 \le X \le 1)$	2D	RPLD	8.0	–	280–330	[17]
$Fe_2O_{3-X}/Cr_{3-X}O_{3-Y}$ (4 layers)	2D	RPLD	15.0	–	280–330	[18]
$Fe_2O_{3-X}/Cr_{3-X}O_{3-Y}$ (2 layers)	2D	RPLD	0.62	420	289–337	[19]

deposition, the reactor was evacuated down to a residual pressure of ~ 4.5×10^{-5} Pa, field up with a flux of pure CH_4 (99.999%) and stabilised to the desired dynamic pressure of 1, 3 and 5 Pa. The Si substrates were first cleaned in an ultrasonic bath with acetone, ethanol and in deionised water and placed parallel at a 45- mm separation distance from Cu targets. Before deposition, the target was cleaned by irradiation with 3000 laser pulses at a fluence of 4.5 J/cm^2 while a shutter was interposed between target and substrate to collect the remnant impurities. The target was rotated at a frequency of 0.5 Hz to avoid piercing and ensure a smooth ablation-deposition process. The ablated and reacted flux of Cu atoms was deposited at room temperature (*RT*) or heated Si substrates, respectively. 2D structures were deposited on high-resistance <100> Si substrates, 0.03 cm thick, having low specific conductivity, i.e. $\sigma \cong 2 \times 10^{-5}/(\Omega$ cm) by 1000–9000 subsequent laser pulses. More details about the setup and the entire experimental scheme are available in our previous papers [17, 19]. We synthesized the 2D structures onto 293, 600 and 800 K Si substrates temperature (T_S) via the reaction of Cu ablated atoms with CH_4 molecules in ambient pressure of 1, 3 and 5 Pa inside the reactor to reach the optimum regime to get the highest values of the *S* coefficient and the photosensitivity *F* too.

2.2 Analysis of the thermo-photosensitivity

The morphology of deposited structures was investigated by scanning electron microscopy (SEM) with Tescan Mira 3 LMU, while the elemental analysis was carried out by energy-dispersive X-ray spectroscopy (EDXS) using JSM-6490 LV JEOL equipment. The structure status of deposited 2D structures was investigated by a Panalytical X'-Pert-Pro-triple-X-ray diffractometer with using Cu ($K_{\alpha 1}$) radiation. The direct current (DC) electrical resistance of deposited 2D structures was monitored by two-probe technique. Ohmic contacts of 2D structures were ensured by silver paste coating or indium coatings. Temperature dependences of the electrical resistance of deposited 2D structures were measured with a high resistance miltimetre. The calculation of specific conductivity (σ) was performed by taking into account structures' thickness (*d*) and the geometrical shape of Si substrate with deposited structure (0.8×0.25) cm^2. The thickness of deposited structures was measured by profilometry with Alpha Step 200 "Tencor Instruments" with an error of 0.4 nm. Structure thickness was measured as step height between Si substrate without any deposits and Si substrate with definite deposits by using Alpha Step 200 "Tencor Instruments" profilometry. The structure thickness is depended on CH_4 pressure in the reactor and Si substrate temperature (T_S).

The optical measurements were carried out by Evolution 220 UV–Visible Spectro photo spectrometer from Thermo Scientific in the range of (190–1100) nm.

The *S* coefficient was investigated within the range of (290–340) K, as this range of temperature is the moderate temperature where the deposited 2D structures demonstrated high thermo-sensitivity depending on the substrate temperature. It should be taken into account that these dependencies were received on nine samples synthesized in the methane atmosphere of $P(CH_4) = 1$, 3, 5 Pa inside the reactor with the deposited 2D structures at different substrate temperature, i.e. $T_S = 293$, 600 and 800. These temperatures were reached by Si substrate heating before laser radiation action on Cu target. A special installation was used to measure the sample temperature and also the temperature difference (ΔT) between heated and *RT* ends of the sample. Two build-in thermocouples were used to this purpose with high thermo conductivity glue. The thermo electro-motive force (emf) (ΔV) was measured between heated and *RT* ends. The temperature dependence of the *S* coefficient was calculated from these data as the ratio $\Delta V/\Delta T$ within the range of (290–340) K after the induction of a thermal gradient along the sample at two definite points.

The photo emf of the deposited 2D structure was measured at *RT* under the irradiation with a source of uniform light intensity in the range of (400–800) nm. Photosensitivity was determined as the ratio between emf (*V*) to incident white light power (*W*), i.e. $F = V/W$, where $V = V_C$ is a "chemical" emf induced in the deposited 2D structures. Uncertainty in a determination of photosensitivity is no more than 2% at *RT* according to root-squared error calculation. It should be mentioned that the average square error was calculated for each point no less than 5 times. Such a low uncertainty is assigned to a high stability of the source generating uniform light intensity within the range of (400–800) nm. The photosensitivity was measured for eight different values of white light power density (W/cm^2). The uncertainty in the determination of the *S* coefficient was no more than 3%. This value is more than the uncertainty in the determination of the photosensitivity owing to higher absolute errors caused by temperature oscillations.

3 Results

3.1 Thermo-photosensitivity properties of 2D structures

The specific conductivity of the deposited 2D structures demonstrated a typical trend for semiconductor materials that can be described by the expression [20]

$$\sigma = \sigma_g \exp\left(-E_g/2k\mathrm{T}\right) + \sigma_i \exp\left(-E_i/k\mathrm{T}\right), \quad (1)$$

where σ_g is the intrinsic conductivity of the 2D structure, σ_i is the conductivity of the 2D structure determined by impurities, k is the Boltzmann constant, E_g is the energy band gap for intrinsic conductivity of the deposited 2D structure and E_i is the band gap assigned to impurities in the synthesized materials (e.g. unreacted copper atoms). In our experimental conditions when $T > RT$, the conductivity σ_g is governed by the main charge carriers, as while structure heating, the impurity concentration is sufficiently less than the intrinsic concentration of charge carriers owing to $E_i < E_g$. Therefore, one can calculate E_g with the following expression:

$$E_g = \frac{2k \ln[\sigma(T_1)/\sigma(T_2)]}{1/T_2 - 1/T_1}, \quad (2)$$

where $\sigma(T_1)$ and $\sigma(T_2)$ are the conductivities at the temperatures T_1 and T_2, when $T_1 > T_2$. The temperature dependence of the specific conductivities of the 2D structure was measured within the range of (290–340) K to check up the semiconductor behaviour of the deposits. The corresponding energy band gap was calculated with uncertainty about 10%. The synthesized 2D structures were deposited on Si substrate at definite methane pressure P(CH_4) and substrate temperature (T_S). The photosensitivity of these structures was investigated and the results are presented in Figs. 1a, 2a, 3a. The influence of specific conductivities on 2D structures' photosensitivity was reviewed. In general, σ temperature dependence exhibits a metal, metal–semiconductor, and semiconductor trend. It was found out that metal or metal–semiconductor dependencies of the σ is characterized by one-two orders of magnitude higher than these values in the case of semiconductor ones. Conductivity σ has a temperature dependence which is similar to that of the behaviour of a semiconductor with the highest photosensitivity (Figs. 1a, 2a, 3a). As it is seen from photosensitivity dependencies, there is saturation for these dependencies at $T_S = 800$ K when increasing white light power density is from 0.04 up to 0.184 W/cm^2.

One notices that the temperature behaviour of 2D structures' specific conductivities is strongly influenced by CH_4 pressure inside the reactor and substrate temperature (Figs. 1b, 2b, 3b). The temperature dependence of the

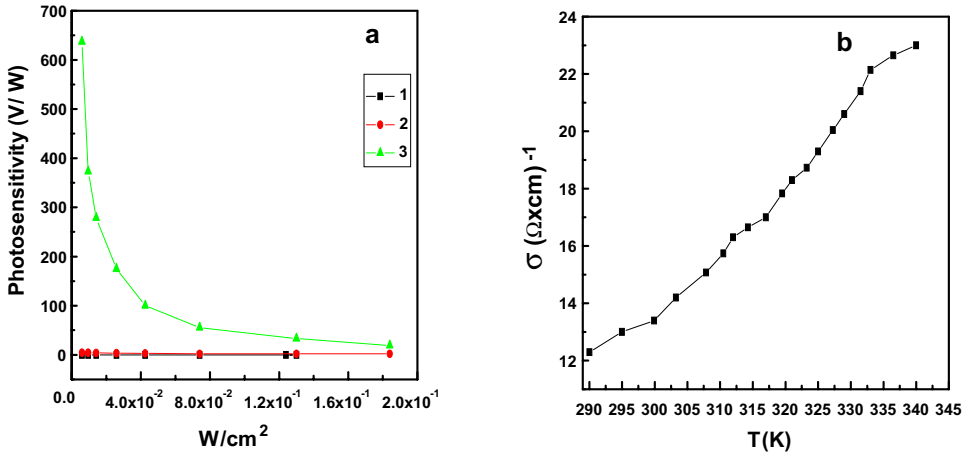

Fig. 1 **a** Photosensitivity of the 2D structure deposited on Si substrate at P(CH_4) = 1 Pa and *Ts* 1—T_S = 293 K; 2—T_S = 600 K; 3—T_S = 800 K, **b** temperature dependence of the 2D structure-specific conductivity at P(CH_4) = 1 Pa and T_S = 800 K

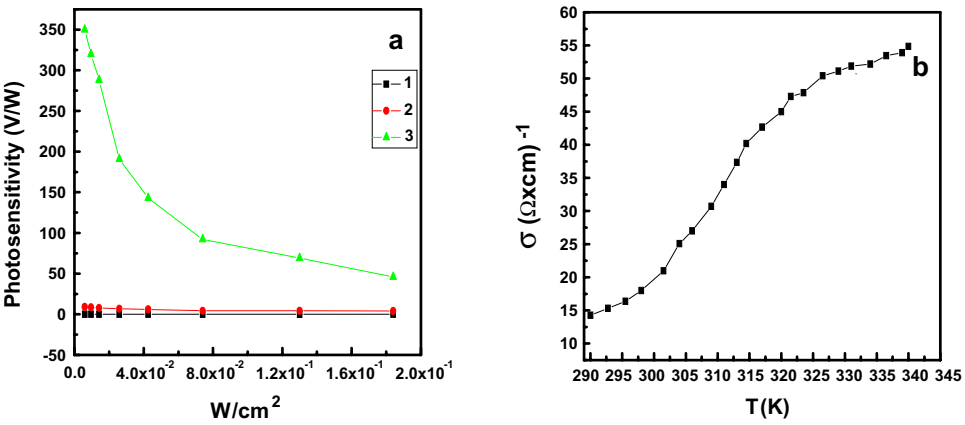

Fig. 2 **a** Photosensitivity of the 2D structure deposited on Si substrate at P(CH_4) = 3 Pa and *Ts* 1—T_S = 293 K; 2—T_S = 600 K; 3—T_S = 800 K, **b** temperature dependence of the 2D structure-specific conductivity at P(CH_4) = 3 Pa and T_S = 800 K

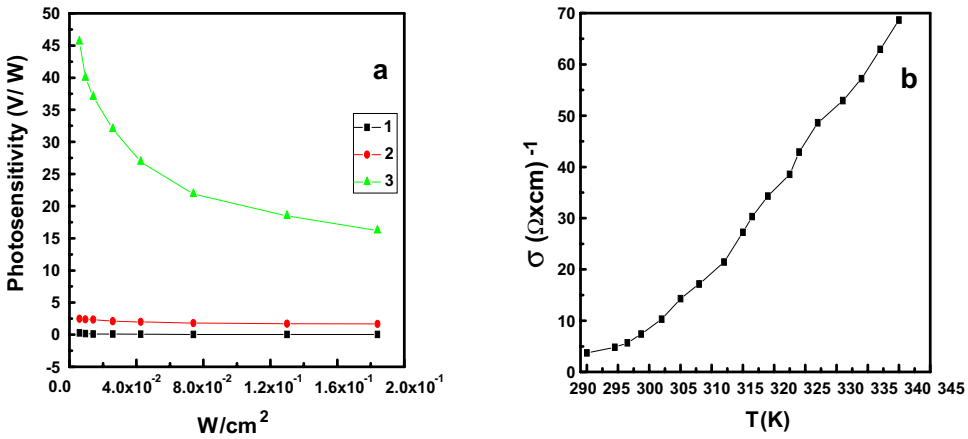

Fig. 3 **a** Photosensitivity of the 2D structure deposited on Si substrate at $P(CH_4) = 5$ Pa and *Ts* 1—$T_S = 293$ K; 2—$T_S = 600$ K; 3—$T_S = 800$ K, **b** temperature dependence of the 2D structure-specific conductivity at $P(CH_4) = 5$ Pa and $T_S = 800$ K

σ exhibits homogeneous semiconductor trend for these 2D structures deposited only on 800 K Si substrate at $P(CH_4) = 1$, 3 and 5 Pa in all temperature range (290–340) K (Figs. 1b, 2b, 3b). Conversely, the 2D structures deposited on Si substrates at 293, 600 K and $P(CH_4) = 1$, 3 and 5 Pa are characterised by metal, semiconductor–metal of the σ trend (Table 2). In general, such a non-homogeneous behaviour of the σ is assigned to the coexistence of two phases inside 2D structures, i.e. semiconductor and metal ones.

The *S* coefficient was measured at $P(CH_4) = 1$, 3 and 5 Pa inside the reactor while element deposition on Si substrate at $T_S = 293$, 600 and 800 K (Table 3). The highest value of the *S* coefficient was obtained for the 2D structure deposited at $P(CH_4) = 5$ Pa and $T_S = 800$ K (Fig. 4).

3.2 XRD, SEM and EDXS analyses of 2D structures

XRD analysis provides information about deposited 2D structures, synthesized under different conditions, i.e. CH_4 pressure inside the reactor and substrate temperature (Fig. 5).

XRD investigations evidenced amorphous 2D structures deposited on 800 K Si substrate (Fig. 5). As it is seen, the deposited 2D structures reveal crystalline phases at $T_S = 293$, 600 K, i.e. Cu (111), Cu (200), Cu (220) and Cu_2O (111) (Fig. 5).

As it is known, the photo emf existence in semiconductors is assigned with heterogeneity concentration of materials along with the deposited 2D structure and with the non-equilibrium of charge carriers' concentration across structure due to light absorption only in a part of the substrate depth, i.e. skin layer ($1/\alpha$), where α is the specific absorption coefficient which is obtained from their transmittance spectra within the range of (400–800) nm (Fig. 6 and Table 2) [21]. Moreover, it is needed to get information about element composition in atomic % concentration of the deposited 2D structures' depth. For example, SEM and EDXS revealed data for the deposited 2D structures at CH_4 pressure of 5 Pa and different T_S. SEM (Fig. 7a,

Table 2 Parameters of the deposited 2D structures on Si substrate at chosen CH_4 pressure and substrate temperature. Energy band gap E_g (eV) = 0 is a characteristic for metal σ trend dependences

CH_4 gas pressure, (Pa)	Si substrate temperature, T_s, (K)	2D structure thickness, *d* (nm)	Skin layer thickness (nm) in the range of (400–800)nm	Temperature range, (K)	Energy band gap, E_g, (eV)
1.0	293	160	–	290–340	0
	600	150	–	290–340	0
	800	140	78–126	290–340	0.21
3.0	293	160	–	290–340	0
	600	150	18–19	290–305	0.94
			–	305–340	0
	800	125	26–16	290–322	0.60
			26–16	322–340	0.17
5.0	293	150	–	290–340	0
	600	110	17–11	290–311	0.74
			–	311–340	0
	800	56	116–476	290–340	1.0

Table 3 Parameters of the deposited 2D structures on Si substrate at chosen CH_4 pressure, substrate temperature and element composition made by EDXS in atomic % without Si atoms' contribution

CH_4 gas pressure, (Pa)	Si substrate temperature, T_s, (K)	F_{max}, (V/W)	S_{max}, (mV/K)	Element composition of 2D structures		
				% C	% O	% Cu
1.0	293	0.06	0.01	68.00	2.67	29.31
	600	4.4	2.10	67.34	5.39	27.25
	800	640	1.35	53.00	15.16	31.89
3.0	293	0.135	0.04	74.04	3.76	22.20
	600	9.0	1.0	58	7.00	35.00
	800	350	1.1	40.31	11.21	48.48
5.0	293	0.25	1.1	50.76	8.54	40.70
	600	2.30	2.7	64.27	4.71	31.02
	800	46	10.5	75.18	12.5	12.32

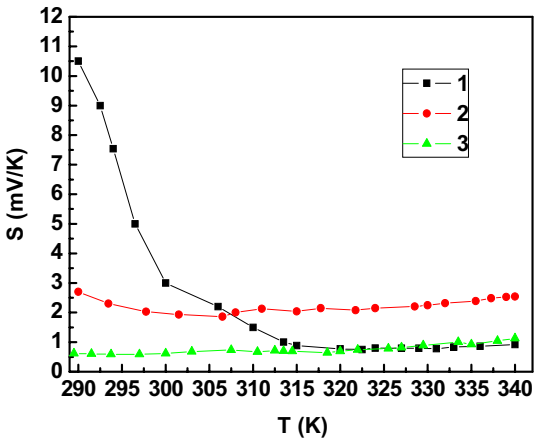

Fig. 4 Seebeck coefficient, S vs. temperature for the 2D structures deposited on Si substrate at $P(CH_4) = 5$ Pa for: 1—$Ts = 800$ K, $d = 56$ nm; 2—$Ts = 600$ K, $d = 110$ nm; 3—$Ts = 293$ K, $\mathbf{d} = 150$ nm

c, e) and EDXS (Fig. 7b, d, f) present the information about the morphology and element composition of these deposits (Table 3). The higher the T_S value, the bigger is the size of the so-called "bubbles" with about 100 nm size associated with metal oxides in 2D deposits which demonstrated mainly metal (1), semiconductor–metal (2) and semiconductor (3) trend for these structures (Figs. 6, 7a, c, e and Table 2). However, the deposited 2D structure at $T_S = 800$ K demonstrated only a semiconductor trend in all CH_4 pressure (Table 2). The morphology influence of these 2D structures on their photosensitivity was investigated too. It was found out that the less "bubbles" size, the less is photosensitivity owing to the increase of Rayleigh light scattering with the decreasing of T_S (Fig.7a, c, e).

The main parameters of the deposited 2D structures are submitted in Tables 2 and 3**.** The important result from these two tables is the 2D structures' metal-like behavior was being changed into an amorphous semiconductor phase when substrate temperature was being increased up to 800 K (Fig. 5).

As it is seen, 2D structure thickness is dependent on Si substrate temperature owing to thermo-desorption of CH_4 molecules resulted in decreasing of structure thickness while increasing of Si substrate temperature. On the other hand, 2D structure thickness is being decreased with gas pressure increasing owing to the collision frequency enlarge of ablated Cu atoms with gas molecules resulted in their kinetic energy loss and, therefore, structure thickness decrease.

4 Discussion

4.1 2D structure's Seebeck coefficient

As it is known, the S coefficient is important when investigating kinetic phenomena of charge transfer in materials [1]. To this purpose, it is essential to analyse the correlation between the temperature and the specific conductivity besides the one between the temperature and the S coefficient of samples. If one starts from the expressions for electron and hole concentrations in a non-degenerate semiconductor, it is possible to express the S coefficient in the form [22]:

$$S = -k/e\left\{\frac{\left[2+\ln(N_c/n)\right]n\mu_n - \left[2+\ln(N_v/p)\right]p\mu_p}{n\mu_n + p\mu_p}\right\}, \quad (3)$$

where k is the Boltzmann constant, e is the electron charge; n, p are electron and hole concentrations; N_c, N_V are effective density of states in the conduction and valence bands and μ_n, μ_p are electron and hole mobility, respectively. This means that the thermo emf coefficient, S, of semiconductor materials is determined by the two parts corresponding to electrons and holes, respectively, as can be inferred from expression (3). The temperature dependence observed for the S coefficient was uniform due to the stability of the

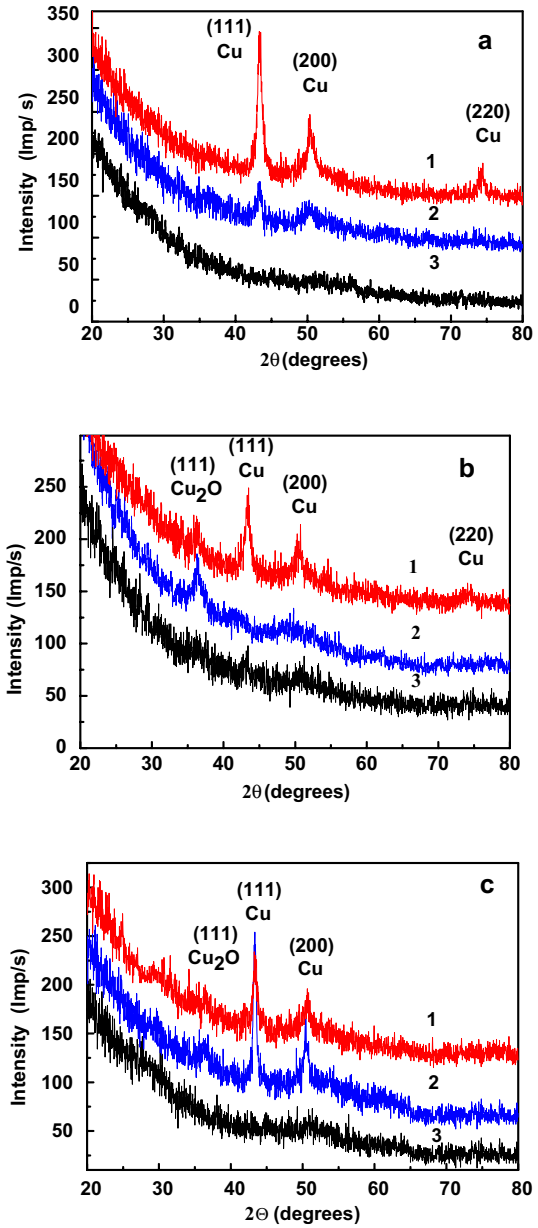

Fig. 5 XRD diagrams of 2D structures deposited on Si substrate at different *Ts* temperatures: 1, 293; 2, 600 and 3, 800 K, respectively and methane pressures inside the reactor **a**—1; **b**—3; **c**—5 Pa, respectively

density of states for valance and conduction bands and for impurity levels in the temperature range of (290–340) K. As it is known, there is a quantum dimension effect in narrow band gap 2D semiconductor [23]. In the case of quasi-pulse periodic Karman-Born conditions, the effective density of N_c and N_v states in 2D zone is proportional to the effective mass of free charge carriers and is equal for 2D structure surface unit [23]

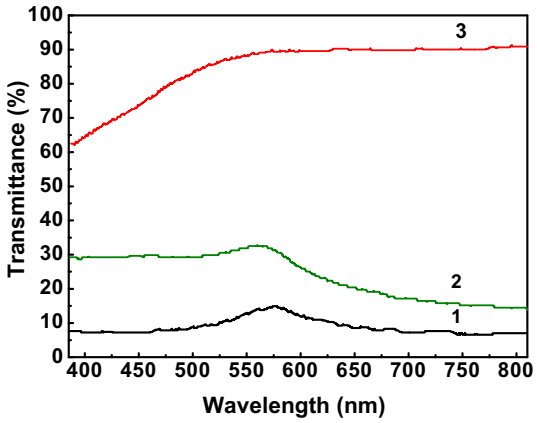

Fig. 6 Transmittance spectra in the range of (400–800) nm for the deposited 2D structures on SiO_2 substrate at $P(CH_4)=5$ Pa and 1—$T_s=293$ K, 2—600 K, 3—800 K

$$N_S = 2\pi \frac{m_p^*}{h^2}, \tag{4}$$

where m_p^* is the effective mass of free charge carriers in 2D structure plate, h is Plank constant.

The density of N_c and N_v states in two-dimensional zone evaluated for 2D structure volume unit can be expressed as [23]:

$$N_V = 2\pi \frac{m_p^*}{h^2 d}, \tag{5}$$

where d is 2D structure thickness. N_V is a function of d and effective mass of free charge carriers. As it is seen from the expression (5), the lower 2D structure thickness, the more effective is the density of states in the conduction and valence bands and higher is the S coefficient. The higher the temperature gradient between either heated and an RT end of the samples, the higher is the gradient of charge carriers' concentration resulted in increasing thermo emf coefficient S (3). On the other hand, the deposited 2D structure at 5 Pa of CH_4 on 800 K Si substrate demonstrated the S coefficient decreasing within the temperature range of (290–315) K (Fig. 4). This effect can be explained with a decreasing display of p-type charge carriers' concentration dealt with the Cu:O ≅ 1:1 stoichiometry that exhibits semiconductor properties (Table 3). When Ts was being increased from 293 to 800 K, the atomic % Cu concentration was being increased in the case of 1 and 3 Pa CH_4 in the deposited 2D structures resulted in only a little increase of the S coefficient. Conversely, decreasing of the atomic % Cu concentration for 5 Pa CH_4 when T_S was increased up to 800 K resulted in a high increase of the S coefficient up to 10.5 mV/K (Table 3, Fig. 4). Moreover, when T_s was decreased a metal-like behavior of the specific conductivity was being appeared

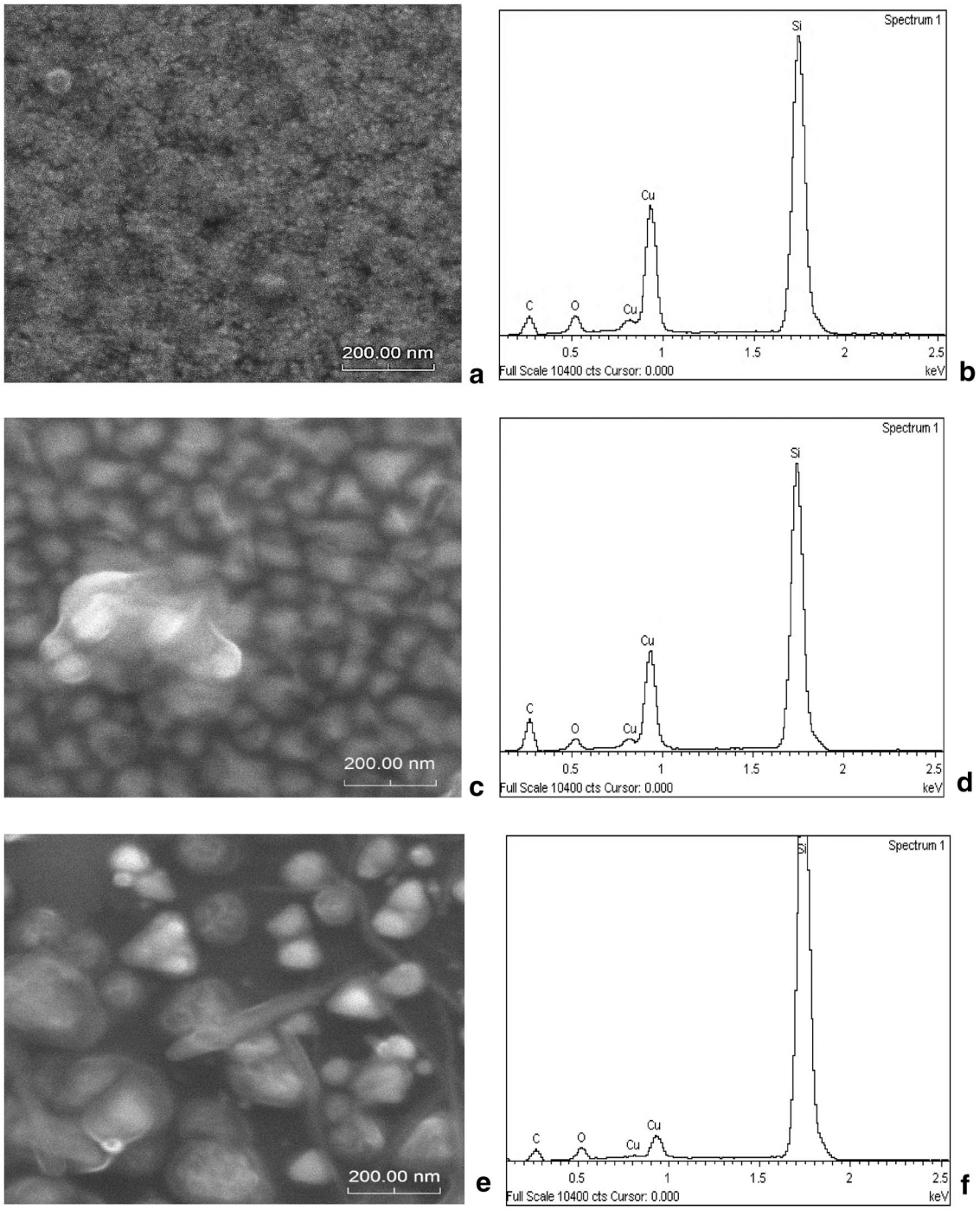

Fig. 7 **a**, **c**, **e** SEM with a scale 200 nm and **b**, **d**, **f** EDXS typical analyses for the deposited 2D structures at Ts = 293 K (**a**, **b**); Ts = 600 K (**c**, **d**); Ts = 800 K (**e**, **f**) and P(CH_4) = 5 Pa

(Tables 2). It should be mentioned, that C atoms act in this experiment similar to a metal one, i.e. the presence of *n*-type charge carriers' resulted in a decrease of the *S* coefficient. In general, the increase of both T_s and CH_4 pressure induced the enhancement of % O atomic concentration inside the deposited 2D structures. Oxygen atoms are mainly created from the natural SiO_2 layer that is on Si substrate surface and promoted these atoms in chemical reactions with Cu atoms flux that hits that surface (Table 3). Results in this paper are obtained on amorphous 2D single-layered structure with high thermo-sensitivity and are based on amorphous phase CuO synthesized by RPLD. Before, high thermo-sensitivity

was exceptionally achieved on the polycrystalline 2D single or multi-layered structures with semiconductor properties synthesized by PLD, LCVD and RPLD [2–4, 7, 12–18].

4.2 2D structure's photosensitivity

In our case, photo emf is due to the existence of concentration heterogeneities of charge carriers along 2D structure and the non-equilibrium distribution of these charge carriers concentration when white light is not absorbed in the entire depth of the structure. Such photo emf is generally described as "chemical" emf because it is assigned with chemical potential (V_C). Therefore, photo emf is induced on the 2D structures when it was irradiated with white light power and grows owing to the photovoltaic effect. It should be noted the higher is the absorption inside 2D structure, the higher is α coefficient resulted in the skin layer decrease (Tables 2). On the other hand, the photosensitivity was higher for narrower band gap semiconductor owing to increasing of white light absorption. It was found out that the higher photosensitivity was for the smallest irradiated area of about 10^{-2} cm^2. This effect could be attributed to the heterogeneities expansion with irradiated area decreasing. The photo emf for any given light exposition of the 2D structure surface can be generally determined with the following expression [21]:

$$V_C = -\frac{kT}{e} \ln \frac{1 + \Delta\sigma_m/\sigma_{01}}{1 + \Delta\sigma_m/\sigma_{02}} \quad (6)$$

where $\Delta\sigma_m$ is the specific conductivities' change under the action of radiation, while σ_{01} and σ_{02} are the specific conductivities in two different points at the absence of any radiation. As follows from the expression (6), the more specific conductivity gradient between the points (1) and (2) exists, the higher photo emf can be induced. As it is known [21], V_c is defined as the energy required for one electron–hole pair generation. For high irradiation intensities, i.e. for $\Delta\sigma_m >> \sigma_{01}$ and $\Delta\sigma_m >> \sigma_{02}$, V_C reaches a saturation value, that is being determined by the gradient of the specific conductivity only, i.e. by the charge carrier concentration. The increase of photosensitivity with substrate temperature increasing can be due to either the skin layer decrease or the increase of heterogeneities concentration owing to their amorphous structures. The highest photosensitivity owing to the highest emf was observed only in the case of amorphous semiconductor structures. As it is seen from Table 2, the higher photosensitivity due to higher non-equilibrium charge carrier's distribution can be explained with the skin layer decreasing in comparison with the deposited 2D structures' thickness. On the other hand, photosensitivity decreasing with the crystalline advent of deposited structures is being explained by heterogeneities decreasing inside the structures (Fig. 5 and Tables 2, 3). Results in this paper are obtained on amorphous 2D single-layered structure with high photosensitivity and are based on amorphous phase Cu_2O synthesized by RPLD. Photosensitivity increasing up to 640 V/W on the amorphous 2D single-layered structure with semiconductor properties is assigned by heterogeneity increasing and the Rayleigh light's scattering decreases while deposition on the heated Si substrate. Before our present studies, high photosensitivity was achieved on the 2D heterostructures with semiconductor properties owing to the synthesized amorphous phase of chromite ($FeCr_2O_4$) on the interphase of iron and chromium oxides' of the polycrystalline 2D single-layered structures synthesized by RPLD [19].

5 Conclusions

Synthesized amorphous 2D single-layered structures by RPLD on oxidized Si substrates in the reaction of Cu atoms with CH_4 molecules exhibit semiconductor properties within a substrate temperature of (290–340) K. Optimum deposition conditions were defined in the relation with the highest thermo-photosensitivity to have been reached in our main experimental conditions, i.e. methane pressure in the reactor, substrate temperature and the thickness of the amorphous 2D single-layered structures. The highest obtained photosensitivity to white light was high as 640 V/W and the highest thermo-sensitivity (Seebeck coefficient) was high as 10.5 mV/K. For the first time, the highest thermo-photosensitivity was achieved on such amorphous 2D single-layered structures with semiconductor properties and the stoichiometry Cu:O ≅ 1:1, Cu:O ≅ 2:1.

Therefore, these amorphous 2D single-layered structures synthesized by RPLD are among of the most promising candidates based on non-toxic precursors for "green" technology fabrication of efficient thermo-photo sensors operating at moderate temperatures. Moreover, RPLD serves as an up-to-date method for the synthesis of amorphous 2D single-layered structures with superior thermo-photo properties.

Acknowledgements N.Stefan and S.A.Mulenko express the gratitude to the support of National Academy of Sciences of Ukraine and Romanian Academy in the frame of the theme "Synthesis of nanostructured and heterostructured materials for sensors and energy converters" and N. Stefan acknowledges the support of Romania National Authority for Research and Innovation (UEFISCDI) under PN 16N/2020 Nucleus Program. S.A.Mulenko and other authors acknowledge the support of National Academy of Sciences of Ukraine to the support of the theme No. 0118U000416 and The State Financed Program "Support for the development of priority arrear of scientific research" KPKVK No. 6541230-3A.

References

1. H.S. Nalwa, *Handbook of Nanostructured Materials and Nanotechnology* (Academic Press, San Diego, 2000), pp. 1–5
2. A.P. Caricato, A. Luches, F. Romano, S.A. Mulenko, Y.V. Kudryavtsev, N.T. Gorbachuk, C. Fotakis, E.L. Papadopoulou, R. Klini, Appl. Surf. Sci. **254**, 1288 (2007)
3. A.P. Caricato, N.T. Gorbachuk, A.M. Korduban, G. Leggieri, A. Luches, P. Mengucci, S.A. Mulenko, D. Valerini, J. Vac. Sci. Technol. B **28**(2), 95 (2010)
4. A.P. Caricato, A. Luches, M. Martino, D. Valerini, Y.V. Kudryavtsev, A.M. Korduban, S.A. Mulenko, N.T. Gorbachuk, J. Optoelectron. Adv. Mater. **12**, 427 (2010)
5. S.A. Mulenko, V.P. Mygashko, Appl. Surf. Sci. **252**, 4449 (2006)
6. A.P. Caricato, Y.V. Kudryavtsev, G. Leggiery, A. Luches, S.A. Mulenko, J. Phys. D Appl. Phys. **40**, 4866 (2007)
7. S.A. Mulenko, N.T. Gorbachuk, Appl. Phys. B **105**, 517 (2011)
8. S.A. Mulenko, Yu.N. Petrov, N.T. Gorbachuk, Appl. Surf. Sci. **258**, 9186 (2012)
9. M. Contreras, L. Mansfield, B.Egaas, J. Li , M. Romero, R. Noufi, E. Rudiger-Voigt, and W. Mannstadt, *in Proceedings of 37 th IEEE Photovoltaic Specialists Conference* (2011), p. 26
10. A. Chirila, Nat. Mater. **12**, 1107 (2013)
11. V. Moise, R. Cloots, A. Rulmont, In. J. Inorg. Mater. **3**, 1323 (2001)
12. H. Ohta, S. Kim, Y. Mune, T. Mizoguchi, K. Nomura, S. Ohta, T. Nomura, Y. Nakanishi, Y. Ikuhara, M. Hirano, H. Hosono, K. Koumoto, Nature Mater. **6**, 129 (2007)
13. T.C. Harman, P.J. Taylor, D.I. Spears, M.P. Walsh, J. Electron Mater. **29**, L1 (2000)
14. Yu Bo, W. Liu, S. Chen, H. Wang, H. Wang, G. Chen, Z. Ren, Nano Energy **1**, 472 (2012)
15. D. Hartung, F. Gather, P. Hering, C. Kandzia, D. Reppin, A. Polity, B.K. Meyer, P.J. Klar, Appl. Phys. Lett. **106**, 253901 (2015)
16. S.A. Mulenko, N.T. Gorbachuk, N. Stefan, Int. Res. J. Nanosci. Nanotechn. **1**(2), 008 (2014)
17. S.A. Mulenko, N.T. Gorbachuk, N. Stefan, Laser Manufact. Mater. Process. **1**, 21 (2014)
18. S. Mulenko, N. Gorbachuk, N. Stefan, F. Miroiu, Front. Sens. (FS) **4**, 16 (2016)
19. S.A. Mulenko, N. Stefan, F. Miroiu, I.N. Mihailescu, N.T. Gorbachuk, V.A. Nikirin, J. Laser Appl. **28**, 042006 (2016)
20. C.A. Wert, R.M. Thomson, *Physics of Solids* (McGraw-Hill Book Company, New York, 1964), p. 556
21. J. Tauc, *Foto and Thermoelectric Affects in Semiconductors* (Pergamon Press, Oxford, New York, 1962), p. 248
22. K.V. Shalimova, *Fizica Poluprovodnikov*, 3rd edn. (Energoatomizdat, Moskva, 1985), pp. 177–181. **(in Russian)**
23. V.F. Kiselev, S.N. Kozlov, A.V. Zoteev, Osnovi fiziki poverhnosti tverdogo tela, (Moskovski Universitet, 1999) p. 284 (in Russian)